

**Mineral composition of Al-rich float rocks in Jezero crater as seen by SuperCam.** C. Royer<sup>1,\*</sup>, C. C. Bedford<sup>1</sup>, R. C. Wiens<sup>1</sup>, J. R. Johnson<sup>2</sup>, B. H. Horgan<sup>1</sup>, A. Broz<sup>1</sup>, O. Forni<sup>3</sup>, S. Connell<sup>1</sup>, L. Mandon<sup>4</sup>, B. S. Kathir<sup>5</sup>, E. M. Hausrath<sup>6</sup>, A. Udry<sup>6</sup>, J. M. Madariaga<sup>7</sup>, E. Dehouck<sup>8</sup>, R. B. Anderson<sup>9</sup>, P. Beck<sup>10</sup>, O. Beyssac<sup>11</sup>, É. Clavé<sup>12</sup>, S. M. Clegg<sup>13</sup>, E. Cloutis<sup>14</sup>, T. Fouchet<sup>15</sup>, T. S. Gabriel<sup>9</sup>, B. J. Garczynski<sup>1</sup>, A. Klidas<sup>1</sup>, H. T. Manelski<sup>1</sup>, L. Mayhew<sup>16</sup>, J. Núñez<sup>2</sup>, A. M. Ollila<sup>13</sup>, S. Schröder<sup>12</sup>, J. I. Simon<sup>17</sup>, U. Wolf<sup>13</sup>, K. M. Stack<sup>18</sup>, A. Cousin<sup>3</sup> and S. Maurice<sup>3</sup> <sup>1</sup>EAPS, Purdue Univ., West Lafayette, IN, USA; <sup>2</sup>JHUAPL, Laurel, MD, USA; <sup>3</sup>IRAP, Toulouse, France; <sup>4</sup>Caltech, Pasadena, CA, USA; <sup>5</sup>Western Washington Univ., Bellingham, WA, USA; <sup>6</sup>Univ. of Nevada, Las Vegas, NV, USA; <sup>7</sup>Univ. of Basque Country, Leioa, Spain; <sup>8</sup>Univ. de Lyon, Lyon, France; <sup>9</sup>USGS, Flagstaff, AZ, USA; <sup>10</sup>IPAG, Grenoble, France; <sup>11</sup>IMPMC/MNHN, Paris, France; <sup>12</sup>DLR, Berlin, Germany; <sup>13</sup>LANL, Los Alamos, NM, USA; <sup>14</sup>Univ. of Winnipeg, Winnipeg, MA, Canada; <sup>15</sup>LESIA, Meudon, France; <sup>16</sup>Univ. of Colorado, Boulder, CO, USA; <sup>17</sup>NASA JSC, Houston, TX, USA; <sup>18</sup>JPL, Pasadena, CA, USA; \*[royer10@purdue.edu](mailto:royer10@purdue.edu)

**Introduction:** During its traverse across the Jezero crater floor and western fan, the *Perseverance* rover encountered > 4000 float rocks – of variable size (up to ~ 50 cm) scattered on the ground without apparent connection to the surrounding stratigraphy [1]. Analysis performed using the SuperCam instrument’s [2, 3, 4] Laser Induced Breakdown Spectroscopy (LIBS) revealed a high concentration of Al<sub>2</sub>O<sub>3</sub>, Cr, Ti and Ni [5], and very low of Fe, Mg, Ca and Na [5, 1]. SuperCam’s infrared reflectance spectroscopy (IRS, between 1.3 and 2.6 μm) showed the presence of Al-rich aqueous alteration minerals (characteristic absorption bands of kaolinite and Al-smectites at 1.4 and 2.2 μm) as well as some (likely Cr-) spinels, identified through their broad asymmetric 2 μm band, responsible for the concavity of IR spectra. These mineral species alone do not fully account for the spectral shapes; hence, the objective is to further investigate spectral modeling to determine the most probable mineral assemblages. Here, we present the results of modeling 17 light-toned float rocks, up to Sol 924, complementary to [1].

**Method:** The modeling method we employed relies on the use of linear combinations of reflectance spectra derived from a library of laboratory spectra. The concept involves blending a large number of spectral *endmembers* to account for the variability of reflectance of each species based on its state (powders of various grain sizes, slabs), observation conditions, and purity. This approach involves several successive steps, using calibrated IRS data [6] of every target.

The selection of endmembers populating the spectral library is based on the preliminary analysis of IR spectra and LIBS data. Here, only species exhibiting absorption bands compatible with observations (1.4, 1.9, 2.2, 2.39 μm) and having very low Fe and Mg, and high Al contents, have been retained by the model: kaolinite, halloysite, Al-phyllsilicates (montmorillonite, illite), Al-hydroxide, hydrated silica (opal-A), spinel, Al-silicate (cordierite), and zeolite. Even though sulfur is not detected *a priori* by LIBS, given its detection threshold close to 10 % [7], sulfates

were included in the library to account for an observed broadening of the 1.9 μm band relative to other candidate minerals.

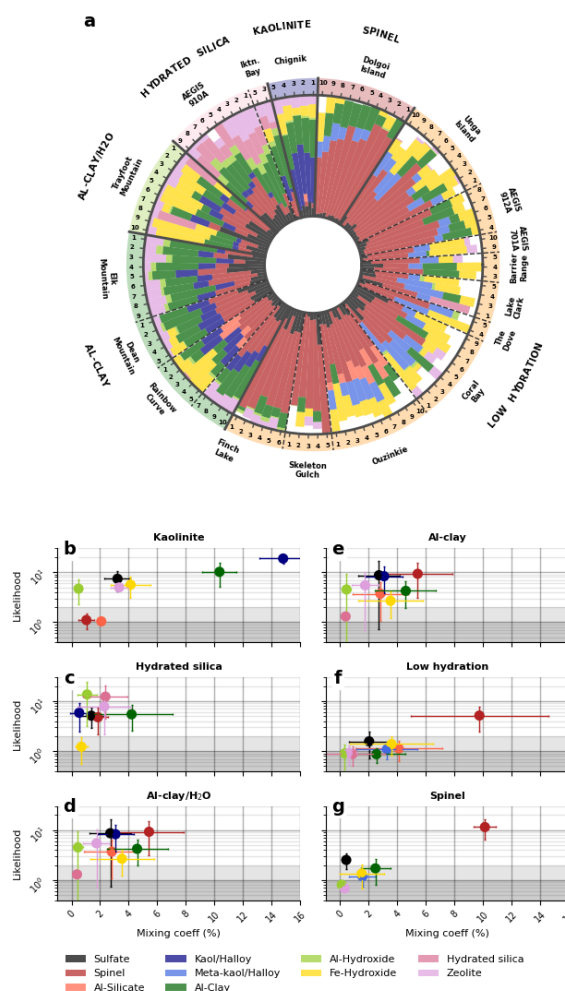


Figure 1: **a:** Representation of the mixing coefficients for each point analyzed on each target by SuperCam. **b–g:** Likelihood as a function of the mixing coefficient averaged over each target cluster. The error bars represent the 1-σ dispersion within each group.

Rocks exhibiting low hydration have been modeled using a dehydrated version of kaolinite and hal-

loysite. Additionally, Fe-hydroxide simulates the thin dust layer covering certain targets. Finally, a correlation filter is applied to the library to eliminate duplicate endmembers more than 99 % similar.

The spectral modeling is then executed in two steps: 1) the spectral assemblage that best fits the data is determined by minimizing the difference between the model and the data, thereby obtaining the set of mixing coefficients corresponding to each mineral family; 2) these coefficients are re-injected into a sensitivity analysis procedure based on a Markov Chain Monte Carlo (MCMC) algorithm to determine the likelihood of each family. This latter parameter represents the sensitivity of the mixture to the presence of a mineral family. If the likelihood is lower than 1, then the presence of that mineral has little impact on the quality of the fit and thus is unlikely to be present.

**Results:** The results of the spectral modeling reveal complex compositions that converge in 6 categories with relatively marked differences (Fig. 1a): 1) The family dominated by kaolinite/halloysite, including only the Chignik target and characterized by doublets at 1.4 and 2.2  $\mu\text{m}$ , indeed exhibits the highest mixing coefficient for these minerals and very high likelihood (Fig. 1b), but also significant influence from Al-clays and sulfates. 2) The family containing Iktan Bay and AEGIS 910A [8] is defined by its strong mixing coefficient for hydrated silica, yet it also presents a plausible portion of Al-hydroxide, sulfate, and zeolite (Fig. 1c). 3) Trayfoot Mountain exhibits a more varied modeled composition, rich in Al-clay, sulfates, Fe-hydroxide, and spinel (Fig. 1d). The latter explains the shape of the spectrum, more concave than it would have been with hydrated phases only. 4) Other hydrated targets share a similar modeled spectrum, rich in Al-clay, sulfate, kaolinite/halloysite, but the spectrally dominant family is spinel, as evidenced by the concave shape of the spectrum. Only Rainbow Curve indicates the presence of cordierite (Fig. 1e) due to its drop in reflectance at 1.4  $\mu\text{m}$ . 5 – 6) The least hydrated rocks form a relatively homogeneous group (Fig. 1f, g), dominated by spinel with varying occurrences of aqueous alteration minerals (metakaolinite/metahalloysite, Al-clay, sulfates). Ouzinkie also exhibits the presence of cordierite, for the same reason as for Rainbow Curve. Dolgoi Island is isolated in a specific spinel-bearing group because of its spectra strongly marked by the broad 2  $\mu\text{m}$  signature.

**Discussion:** The modeling of IR spectra reveals the presence of a wide range of alteration phases associated with high Al-enrichment, but it does not account for the existence of other minerals that do not show signatures in the near-IR, such as glass, mulite, kyanite/sillimanite/andalusite. However, their

presence is probable based on textural and geochemical interpretations. Similarly, it's important to note that the mixing coefficients obtained through modeling only represent the *spectral weight* of each mineral, and the link with quantitative composition is more complex and indirect. The significant presence of spinel in all observations results from the overall concavity of the spectra, which cannot be explained by alteration minerals like clays and hydroxides. However, this mineral forms at high temperature, and its coexistence with hydrated minerals, stable at low temperature, may appear contradictory. Its presence might indicate a complex formation and evolution process, such as non-uniform heating and partial melting of rocks. Multiple scenarios of formation, alteration, and dispersion within Jezero crater could account for such compositions [9, 1]. The scenario we have considered is divided in three main stages: 1) A primary parent rock (basaltic or felsic) would have undergone intense surface aqueous leaching, progressively removing the most soluble ions (Fe, Mg, Ca, Na, K) and transforming primary minerals into phyllosilicates until forming a kaolinite-rich horizon. 2) An intense thermal episode would have occurred after the alteration profile formation (magmatic intrusion, thick lava flow), heating the rocks to over 1000°C, leading to the dehydration of clays, potentially partial melting and formation of metamorphic phases. 3) Finally, erosion or impacts would have fragmented the outcrop, dispersing rock fragments within Jezero, potentially briefly transported by flowing water or ice. In the watershed, several impact craters are associated with kaolinite weathering horizons [10], and light-toned linear features with fractured margins [11] may be potential parent outcrops for these float rocks.

**Conclusion:** These light-toned float rocks stand out among the other rocks and soils comprising Jezero crater. Their exceptionally high Al-content marks them as the most altered rocks ever observed *in situ* on Mars, and the evidence of spinel along with mineral phases associated with intense heating provide the first observational evidence of high-temperature, low-pressure pyrometamorphism on Mars.

#### References:

- [1] C. Bedford et al. *this meeting* (2024).
- [2] R. C. Wiens et al. *Space Sci Rev* 217.1 (2021), p. 4.
- [3] S. A. Maurice et al. (2021).
- [4] T. Fouchet et al. *Icarus* 373 (2022), p. 114773.
- [5] O. Forni et al. *this meeting* (2024).
- [6] C. Royer et al. *Journal of Geophysical Research: Planets* 128.1 (2023).
- [7] R. B. Anderson et al. *Spectrochimica Acta Part B: Atomic Spectroscopy* 188 (2022), p. 106347.
- [8] P. Beck et al. *this meeting* (2024).
- [9] C. Royer et al. *Sci. Adv. (in review)* (2024).
- [10] J. Carter et al. *Icarus* 248 (2015), pp. 373–382.
- [11] M. S. Bramble et al. *Icarus* 293 (2017), pp. 66–93.